Biophysical Chemistry 13 (1981) 49–54
North-Holland Publishing Company

DYNAMIC KERR EFFECT MEASUREMENTS ON PHOTORECEPTOR DISK MEMBRANE VESICLES

Hideo TAKEZOE [1] and Hyuk YU [2]
Department of Chemistry, University of Wisconsin, Madison, Wisconsin 53706, U.S.A.

Received 3 June 1980

Dynamic Kerr effect measurements were performed with dilute aqueous suspensions of monodisperse spherical vesicles (~1 μm diameter), isolated from the rod outer segment of bovine retina. A large birefringence, amounting to the specific Kerr constant of 10^{-3} esu, can be observed. When a sufficiently long duration pulse (1 s) is applied, the decay of birefringence can be represented by a single exponential profile, yielding a relaxation time of 100 ± 20 ms in 1 mM imidazole buffer. This is consistent with the rotatory relaxation time of these spherical membrane vesicles. When a short duration is applied, the birefringence increases more steeply and the decay profile contains several components. The slowest (terminal) relaxation time is 86 ± 15 ms and is due to the same process as the one observed in the slow pulse case.

1. Introduction

The dynamic Kerr effect (DKE) has been used successfully as a powerful tool for investigation of the electric and optical properties of macromolecules in dilute solution. Specifically for rodlike macromolecules, there exists an extensive literature [1]. In the ideal case, i.e., monodisperse and dilute solution, the decay of birefringence can be represented by a single exponential, whose time constant τ is related to the rotatory diffusion constant Θ as $\tau = 1/6\Theta$. Hence, DKE measurements have been used for determination of macromolecular shape and size through the rotatory diffusion constant. In this regard, DKE constitutes one of many hydrodynamic methods for molecular characterization.

Recently, our laboratory has been involved in the study of structure and dynamics of spherical vesicles formed from the photoreceptor disk membranes of rod outer segment (ROS) of bovine retinae. It has been established that these membrane vesicles could be isolated intact from ROS and swollen into monodisperse spherical vesicles of 450–500 nm in radius [2,3] in low osmolar media (mM). Further, not only are they osmotically active [4] but also electrically active by exhibiting a well-defined electrophoretic mobility [5]. Thus the electric field induced birefringence transient technique, DKE, is a natural choice for probing their dynamics and perhaps even that of the photopigment on the membrane surface. There are two specific intramembrane dynamic processes of photopigment hitherto examined by various techniques; they are the lateral translational diffusion [6–9] and the rotatory diffusion [6,10] about the transverse axis of the disk, of rhodopsin, the photopigment which constitutes nearly one-half of the total integral membranous substances [11]. We ask the question: Is the DKE technique amenable to probing one of these processes within spherical vesicles? If the vesicles remain spherical but the uniform distribution of photopigment (and/or phospholipid, the other principal component) can be perturbed by a dipolar electric field, then one should observe a substantial birefringence, even if the perturbation is small, because of the size of these vesicles. Similarly, a field-induced vesicle deformation without attendant redistribution of photopigment (and/or phospholipid) could give rise to the same observation. Thus the DKE technique may be employed for examination of vesicle dynamics,

[1] On leave from Department of Textile and Polymeric Materials, Tokyo Institute of Technology.
[2] To whom correspondence should be addressed.

though interpretation in terms of the specific processes referred to above may be difficult. This was the motivation which has prompted us to examine the DKE of these vesicles. In this paper, we present our first set of experiments which demonstrates conclusively that the DKE technique can appropriately be employed for extraction of at least one dynamic property of the gross vesicle structure, namely the rotatory diffusion constant of vesicles. In addition, it poses a number of intriguing questions, including the exact origin of the enormous birefringence.

2. Experimental procedure

2.1. Samples

Bovine ROS disk membranes were isolated and purified from dark-adapted frozen retinae (American Stores Packing Company, Lincoln, Nebraska) by a modified version [2] of the method originally employed by Smith et al. [12]. The swollen membrane vesicles were suspended in 1 mM imidazole buffer, and the pH of the suspension was monitored at 6.3–6.9 throughout each experiment. Each suspension had 0.1 mM EGTA, which appears to reduce free cation concentration; a small amount of free cations enormously diminishes the birefringence. The vesicle number density was determined by measurement of the optical absorbance at 633 nm, which had earlier been calibrated against a number density determination by viscometry [13]. Thirty-five independently prepared ROS samples were used in this study.

2.2. Dynamic Kerr effect measurements

The optical system of our Kerr effect apparatus is a standard one. The transmitted light transient of 7 mW He/Ne laser was detected by a PMT (RCA C7164R) after being passed through a sample cell placed between a pair of crossed Glan-Thompson prisms. We sometimes used a quarter-wave ($\lambda/4$) plate tuned to 632.8 nm (Karl Lambrecht, Chicago, IL) placed between the cell and the analyzer in order to enhance the signal to noise ratio [14]. The output signal was sent to a transient recorder (Biomation, Model 802), and its digital output was accumulated on a microprocessor computer (Kim I, MOS Technology, Norristown, PA). The averaged result of the transient signal from the microcomputer was output for analysis.

The electric field was applied in a sequence of rectangular pulses with use of a capacitor discharging circuit and a pulse generator. The pulse height, pulse duration and pulse period were all variable. The range of field strength employed was 5–1000 V/cm. The range of pulse duration and pulse period were respectively 5–1000 ms and 1–10 s.

Pyrex glass tubing (1.8 cm dia × 20 cm length) with a pair of low stress optical coefficient flats serving as the windows at both ends was used as the Kerr cell. Platinum plate electrodes (0.4 cm × 12 cm), firmly embedded in a cylindrical KEL-F electrode holder (1.8 cm dia × 12 cm length), were in turn inserted into the glass tube. The separation of the electrodes was 4 mm and the length was 12 cm.

The experiments were performed in the dark at room temperature (293 K). No specific temperature control of the Kerr cell was effected. Since the vesicles tend to aggregate, particularly at higher concentrations, the experiments were performed within three hours after each sample preparation. The sample quality also seemed to be degraded by the long term application of high field; therefore the measurements for a fresh sample were completed within ten minutes after starting to apply the field.

2.3. Calibration of instrument

The calibration of our instrument has been effected by application of an exponentially decaying electric field and monitoring of the resulting birefringence transient of nitrobenzene; nitrobenzene was chosen because its rotatory relaxation time of 30 ps [15] is much faster than the relaxation time of the applied field. Since the induced birefringence Δn is proportional to the square of applied field E, while the optical retardation δ is proportional to Δn, the relaxation time of δ should be faster than that of the applied field E by a factor of two;

$$E = E_0 \exp(-t/\tau), \tag{1}$$

$$\delta = \delta_0 \exp(-2t/\tau). \tag{2}$$

The observed optical intensity from the PMT is related to the retardation as

$$\Delta I = \tfrac{1}{2} I_0 (1 - \cos\delta) \tag{3}$$

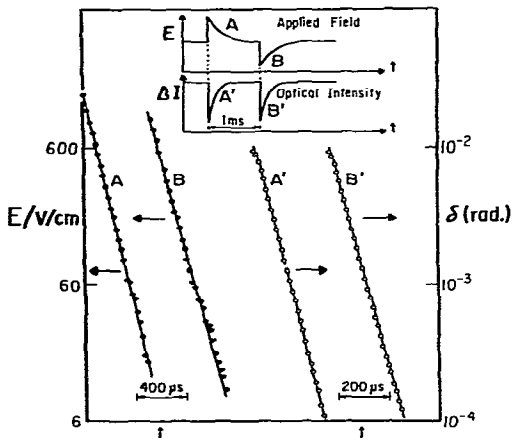

Fig. 1. Logarithmic plots of the applied electric field strength and the birefringence transient due to nitrobenzene. The time axes are scaled in a 2 : 1 ratio. The signal profiles are shown in the upper part.

in the system without a λ/4 plate, or as

$$\Delta I = \tfrac{1}{2} I_0 [\sin(2\theta - \delta) - \sin 2\theta] \qquad (4)$$

in the system with a λ/4 plate, where θ is the polarization axis of the analyzer relative to that of the electric field. We show in fig. 1 how these expectations are borne out by our instrument. Experiments were performed in the system with a λ/4 plate. The filled circles refer to the applied field and the open circles to the optical retardation. The time axes are scaled in a 2 : 1 ratio, so that all four lines should be parallel to each other. This is clearly the case.

3. Results and discussion

A typical birefringence transient is shown in fig. 2, where both the rise and decay profiles of the birefringence are displayed in linear and logarithmic scales. The experimental condition of these runs with a λ/4 plate was 1 s for the pulse duration, 10 s for the pulse period and 5.3 V/cm (filled circles) or 19 V/cm (open circles) for the field strength. The concentration of membrane vesicles was 4.8×10^9 vesicles/cm^3. The birefringence reaches the asymptotic values δ_0, which are 6.9×10^{-4} and 8.3×10^{-3} in radians, respectively.

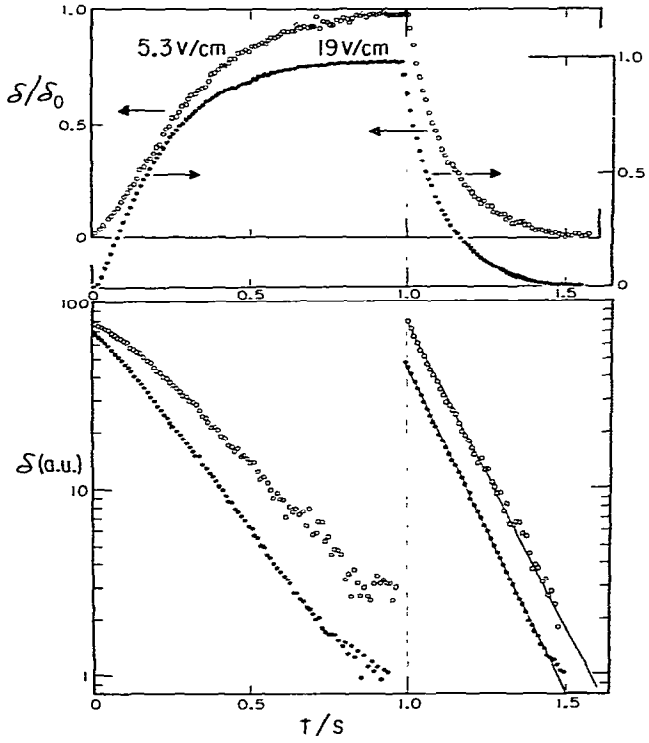

Fig. 2. Linear and logarithmic plots of typical birefringence transient induced by a 1 s duration pulse. The filled and open circles refer to the results for 5.3 V/cm and 19 V/cm field strength, respectively.

It is clear from the lower part of the figure that the decay profiles are well represented by a single exponential and are independent of the field strength. The deduced relaxation time is 100 ± 20 ms. As for the rise portion, it depends on the field strength even in low field regions such as 19 V/cm as shown in the figure. This is due to the saturation effect, as expected by comparison of the two asymptotic values of birefringence and field strength applied.

An additional noteworthy point is that the specific Kerr constant K_{sp} was estimated to be at least on the order of 10^{-3} esu, although a more precise determination of K_{sp} was prevented by the gradual decrease of the signal intensity as we applied sequential pulses. We attribute the decrease to electrophoretic migration of the vesicles toward one of the electrodes

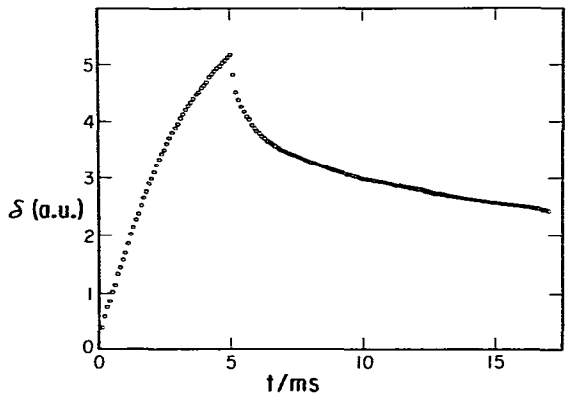

Fig. 3. Typical birefringence transient induced by a 5 ms duration pulse.

as the pulse sequence is cumulatively applied, since we can recover a part of the signal decrement by shaking the cell. The specific Kerr constant on the order of 10^{-3} esu is to be compared with 1.36×10^{-3} esu for tobacco mosaic virus (TMV) in distilled water [16] and 1.3×10^{-5} esu for poly(γ-benzyl-L-glutamate) (M.W. 3.5×10^5) in ethylene dichloride [17], both rigid rod-like dipolar molecules, and with 8.7×10^{-14} esu for polystyrene (M.W. 2.5×10^5) in carbon tetrachloride [18], a flexible random coil molecule with a small permanent dipole moment. We emphasize here that the K_{sp} of the ROS membrane vesicles is comparable to that of TMV, whose linear dimension of 0.3 μm is about the same as 0.5 μm for the vesicle radius.

In fig. 3 is displayed another birefringence transient profile observed under a very different (much shorter) pulse width and (much stronger) field strength than that shown in fig. 2. Here the pulse width was 5 ms, the pulse period 2 s and the field strength 880 V/cm. The rise and decay profile are not symmetric; the rise portion is very sharp and the decay portion is no longer single exponential in profile. The difference

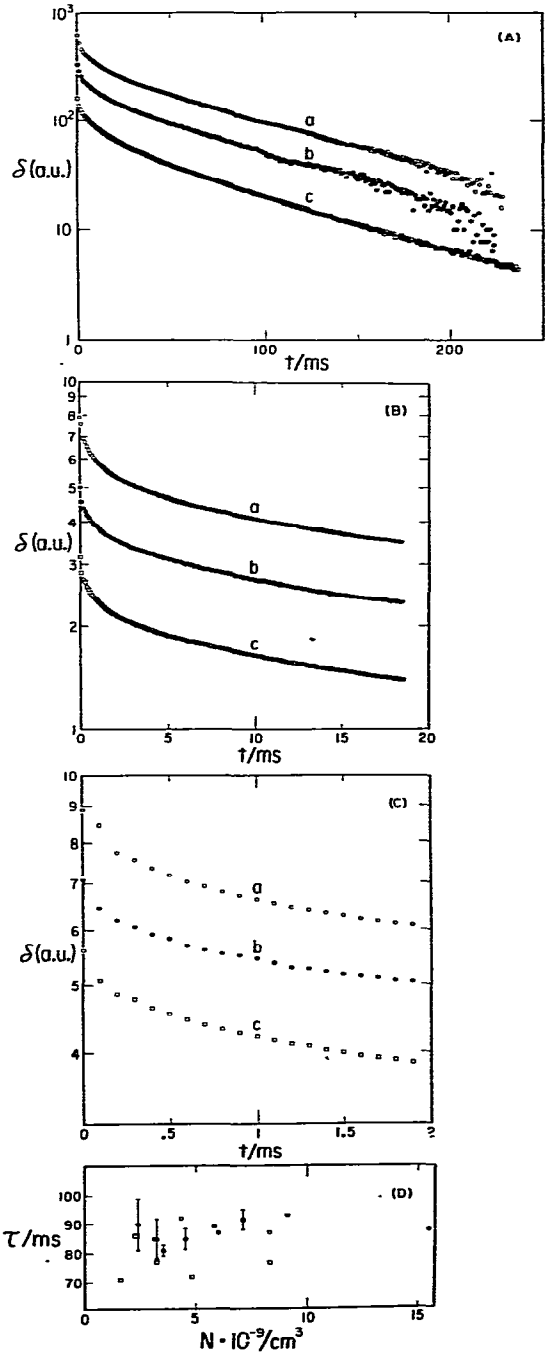

Fig. 4. Logarithimic plots of birefringence transient induced by a 5 ms duration pulse. Data acquisition conditions are listed in table 1. Concentration dependence of the terminal relaxation time is shown in (D). The three independently prepared samples are distinguished by different symbols. The applied fields are 875 V/cm (filled circles), 890 V/cm (open squares) and 1000 V/cm (open circles).

Table 1
Data acquisition conditions referring to fig. 4

		Concentration (vesicles/cm^3)	Field strength (V/cm)	λ/4 plate	Number of acumulations
(A)	a	7.14×10^9	875	w/o	100
	b	3.22×10^9	888	w/o	20
	c	3.87×10^9	750	w/	20
(B)	a	18.90×10^9	1000	w/o	100
and	b	2.09×10^9	750	w/o	20
(C)	c	4.36×10^9	925	w/o	20

from the earlier one is quite striking. The decay profile seems to contain a number of faster relaxation mechanisms beyond $\tau \approx 100$ ms, which were evidently obscured in the long pulse width experiment. This point is amplified graphically in fig. 4 (A), (B) and (C), where the time axis is successively expanded by by one decade each in (B) and (C). The data acquisition conditions are listed in table 1. All three runs are made with separately prepared samples. These plots show the extent of reproducibility of the experiment. The longest time frame decay profiles, shown in fig. 4 (A), represent the slowest (terminal) relaxation mechanism. We should note that there is no concentration dependence of the terminal relaxation time within the number density range of $(1.6-15.5) \times 10^9$ vesicles/cm^3 examined in this study; this is shown in fig. 4 (D). Variability of the terminal relaxation time τ is within 20%, and τ is determined as 86 ± 15 ms, which is in good accord with the result of the long pulse width experiment discussed above.

We now turn to the question of the mechanism for the terminal relaxation. We propose that it is the rotatory diffusion of the spherical vesicles. The relaxation time of a spherical particle with radius r suspended in a medium of viscosity η is

$$\tau = 4\pi\eta r^3/3kT, \qquad (5)$$

where kT has the usual meaning. From the observed $\tau = 86 \pm 15$ ms in the short duration and $\tau = 100 \pm 20$ ms in the long duration case and $\eta = 1.00$ centipoise, we compute the radius r as 0.44 ± 0.02 μm from the short duration case and 0.46 ± 0.03 μm from the long duration case, which is in excellent agreement with the values obtained by elastic light scattering, 0.48 ± 0.06 μm [2,4], and by quasielastic light scattering, 0.51 ± 0.05 μm [2–4]. Eq. (5) also suggests that the terminal relaxation time should be proportional to the solvent viscosity η. By increasing the viscosity with high molecular weight Dextran (M.W. 70 000, Sigma), we confirmed that this is almost the case up to 2.5 centipoise, though a simple proportionality was not obeyed above $\eta = 2.5$ cp. However the concentration of Dextran required to reach such a viscosity is also suspected to deform osmotically the membrane vesicles away from the spherical shape. Thus until the deformation characteristics of the vesicles by Dextran is sorted out, the observed departure from the linear dependence of τ on η needs to be examined further, rather than taking it as evidence contrary to the expectation of eq. (5).

Turning to the multiple exponential profile obtained with short pulse width and high field strength, we note first that the decomposition into a set of three components is possible. This is shown in fig. 5, where the three components are distinguished by their respective relaxation times as 88 ms, 10 ms and 1 ms. The slowest one corresponds to the rotatory diffusion motion of a whole vesicle as discussed above. Where the other two processes come from, we cannot be certain at this time. Neither are we sure of the uniqueness of our decomposition scheme. What we are sure of is that the short pulse width experiment does give rise to the correct terminal relaxation. It is also possible that there may be even faster birefringence decay processes than that given by the 1 ms relaxation time, though the precision of our data precludes us from extracting them .

We have also observed a remarkable effect of divalent and trivalent cations in the vesicle suspensions. Upon addition of a small amount (~100 μM) of $CaCl_2$, $CeCl_3$ or $LaCl_3$, the induced birefringence disappears

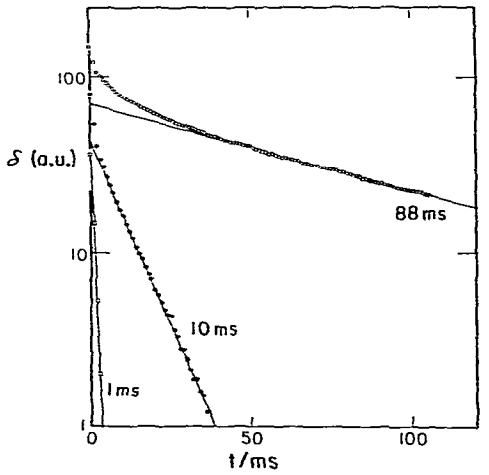

Fig. 5. Decomposition of the birefringence transient induced by a 5 ms duration pulse.

immediately. Inasmuch as these cations are known to bind to the vesicle surface [5], it is not surprising that the vesicles no longer respond to the imposed electric field as before the addition of these cations. Thus it appears that the field induced birefringence requires surface charges, possibly negatively charged groups of the photopigment that is on the extravesicular side. We therefore tentatively propose that the cause of the large birefringence is the field induced perturbation of the random distribution of photopigment (and/or phospholipid) over the spherical surface. Upon removal of the field their return to the unperturbed random distribution would proceed at such a rate that its time constant should be faster than that of the overall vesicle rotatory motion. Possibly this may lie in the range of 1–10 ms as shown in fig. 5. On other words, there should be two distinct sets of processes responsible for the birefringence, namely, the intravesicular polarization process and the overall orientation process. The two sets of the processes are comparably contributing to the birefringence in the short pulse duration experiment whereas the orientation process is dominant in the long pulse duration experiment. This could explain why we obtain multiple exponential profiles in the short duration case and single exponential profiles in the long duration case. The concept of membrane fluidity [19] seems to us to be intimately connected with the intravesicular polarization process, and to the best of our knowledge, O'Konski is the first one to undertake a study of this sort with phospholipid vesicles [20].

Acknowledgements

This work is supported in part by an NIH grant, EY01483, and a Biomedical Sciences Support Grant of NIH administered through the Graduate School of the University of Wisconsin-Madison. We are most grateful to Dr. Eve Marchal who has provided us with a valuable suggestion concerning the calibration of the instrument. We also thank Eric J. Amis who has interfaced the microcomputer to the transient recorder, and Robert W. Schmelzer for his superb craftsmanship in constructing the Kerr cell. We acknowledge brief but most helpful comments by Prof. H. Benoit.

References

[1] C.T. O'Konski, Molecular electro-optics (Marcel Dekker, New York, 1976).
[2] T. Norisuye, W.F. Hoffman and H. Yu, Biochemistry 15 (1976) 5678.
[3] W.F. Hoffman, T. Norisuye and H. Yu, Biochemistry 16 (1977) 1273.
[4] T. Norisuye and H. Yu, Biochim. Biophys. Acta 471 (1977) 436.
[5] G.B. Caflisch, Ph.D. Thesis, University of Wisconsin, 1979;
G.B. Caflisch and H. Yu, to be published.
[6] M. Edidin, Ann. Rev. Biophys. Bioeng. 3 (1974) 179.
[7] M. Poo and R.A. Cone, Exp. Eye Res. 17 (1973) 503.
[8] M. Poo and R.A. Cone, Nature (London) 247 (1974) 438.
[9] P.A. Liebman and G. Entine, Science 185 (1974) 457.
[10] R.A. Cone, Nature (London), New Biol. 236 (1972) 39.
[11] F.J.M. Daemen, Biochim. Biophys. Acta 300 (1973) 255.
[12] H.G. Smith, Jr., G.W. Stubbs and B.J. Litman, Exp. Eye Res. 20 (1975) 211.
[13] E.J. Amis, D.A. Davenport and H. Yu, to be published.
[14] C.T. O'Konski and B.H. Zimm, Science 111 (1950) 113.
[15] D.R. Bauer, J.I. Brauman and R. Pecora, J. Am. Chem. Soc. 96 (1974) 6840.
[16] C.T. O'Konski, K. Yoshioka and W.H. Orttung, J. Phys. Chem. 63 (1959) 1558.
[17] S. Krause and C.T. O'Konski, Biopolymers 1 (1963) 503.
[18] C.G. LeFevre, R.J.W. LeFevre and C.M. Parkins, J. Chem. Soc. 1958 (1958) 1468.
[19] S.J. Singer and G.L. Nicolson, Science 175 (1972) 720.
[20] C.T. O'Konski, in: Transport in Proteins, eds. G. Blauer and H. Sund (Walter deGruyter, New York, 1979) p. 231.